THD improvement of a PWM cascade multilevel power inverters using genetic algorithms as optimization method

JORGE LUIS DIAZ RODRIGUEZ, LUIS DAVID PABON, ALDO PARDO GARCIA.
Faculty of Engineering and Arquitecture
University of Pamplona
Ciudadela Universitaria, Km. 1 via Bucaramanga, Pamplona
COLOMBIA
jdiazcu@unipamplona.edu.co, davidpabon@unipamplona.edu.co, apardo13@unipamplona.edu.co

Abstract: - This paper presents an optimization of the electric power quality by designing a 9 steps multilevel power inverter, which adopts a multi-PWM optimized using genetic algorithms (GA), and minimizing Total Harmonic Distortion (THD) of the first 50 harmonics to about 0%. This optimization is considered an alternative technique because it reduces the expression used to quantify TDH numerically. Particularly for the 9 steps multilevel wave form, it reduces the number of power on-and-off angles as well as the position within the levels of the first quarter-wave modulation. The research involved developing a prototype for experimental verification.

Key-Words: - Multilevel inverter, total harmonic distortion, genetic algorithm, PWM.

1 Introduction

Power quality in photovoltaic (PV) systems depends on the power inverter [1], which is responsible for making a DC / AC conversion, and solar panels generate DC voltage component and conversion is needed to ac for use energy or connect to the network [2]. However, conventional power inverters have some quality problems due to harmonic distortion [3], [4].

To be able to solve this problem, it has been suggested to use multilevel inverters [5], [6] which have lower harmonic content than conventional inverters regarding the output voltage [7], [8]. This research found harmonic content optimization of PV systems through evolutionary techniques using a two-steps multilevel power inverter -for economic reasons- and with the highest number of steps in the output, for this case the number of steps will be nine using cascaded H bridge multilevel inverter with common source topology [9], [10].

2 Multilevel Inverters

The first multilevel inverter was presented by Baker and Lawrence in 1975 [11], called the serial inverter cascade H-bridge topology , in the year 1981 the first multilevel inverter was implemented in three steps through clamping diodes [12], based on this patent and this work it has been generated a variety of researches seeking to optimize and improve the multilevel inverter system [13], one of these proposals is to use a single voltage source directly accompanied by transformers at the output of the H bridge, this topology is the cascaded multilevel inverter H bridge with common source [14]. This configuration is very suitable due to its low cost, renewable energy applications because there is a single power supply for the entire system, however, using output transformers can create problems such as disruption of the waveform and the system becomes more complex [14], [15].

In this research a prototype has been designed based on a methodology proposed by the authors to improve the transformers response in this application [16]; the improvement was shown in the results.

Regarding multilevel inverters modulation, specifically talking about harmonic content optimization, it has been suggested several techniques depending on the topology being used, the specific objective and the way of searching the best point [8], [17]-[22], nevertheless, there are promising strategies in the field of evolutionary algorithms such as Particles Swarm Optimization (PSO), [23], [24] and Genetic Algorithms (GA) [9], [20], [25], for which it has been compared with the common techniques, some of this research has concluded that genetic algorithms gets better results [26], this way, the technique used in this research are genetic algorithms justified in the numeric character of the optimization.

3 Cascade Multilevel Inverter

In figure 1 it shown the general scheme of a Cascade H bridges Multilevel Inverter (*CMLI*) is shown, where the basic performance is presented and in which the output waveform is constructed by adding the outputs of each H-bridge [12].

The CMLI topologies can be divided into two categories depending on the voltages that supply each bridge; therefore these can be symmetrical or asymmetrical. CML is symmetrical when all of them are equal; and asymmetric if the voltages are different, they are common relations 1:2 or 1:3.

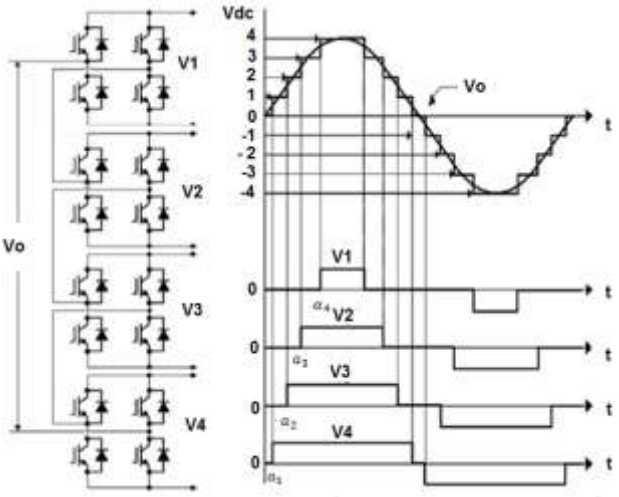

Fig. 1. Cascaded H bridge multilevel inverter, voltage output on the bridges and inverter.

In order to obtain the voltages for each bridge two topologies will be described, first, the independent sources in which all the bridges are powered autonomously (see Figure 2a) and second the common source topology, in the all bridges are powered by a single source where the potential difference and the electrical galvanic isolation is achieved by transformers (see figure 2.b). The figure 2 shows an example of asymmetric form topology with a ratio of 1:2. Both get the same output voltage waveform [10].

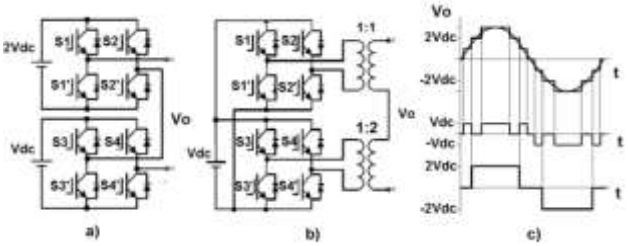

Fig. 2: Topologies of asymmetric cascade H bridges multilevel inverter. a) Independent source. b) Common Source. c) Output voltage.

3.1. Multilevel Inverter common source of three stages

The multilevel inverter topology selected for this work is the cascade H bridge multilevel inverter asymmetrical common source with 1:3 ratios of 2 steps, which generate 9 levels of output voltage.

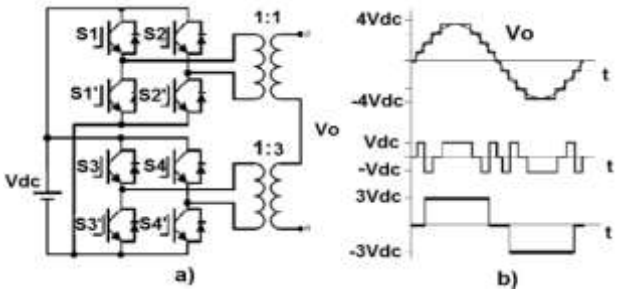

Fig. 3. Asymmetric Cascade Multilevel Inverter common source, two stages with 9 levels at the output, asymmetry 1:3. a) Topology. b) Output voltage.

This inverter allows with minimal H bridge stages (2 steps) to reach the maximum number of steps in the output voltage (9 steps). In fig. 3 shows how the selected topology and the generated voltage is observed.

4 Mathematical Modeling

The waveform of a multi-modulation PWM to 9 steps is shown in Figure. 4.

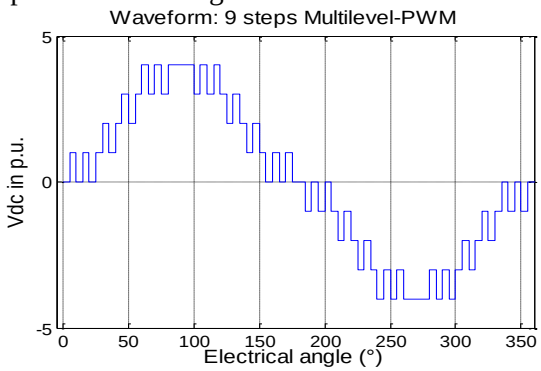

Fig. 4. Waveform output voltage PWM 9 steps.

In this research it was obtained an expression that quantifies the total harmonic distortion with reference to the number of switch angles on and off (firing angles) for each step.

The modulation form has a ¼ wave symmetry so it is necessary to define these angles in the first quarter-wave only (fig. 5); the remaining modulation was constructed by using trigonometric relationships. Thus, a vector $L = [x\ y\ z\ w]$ which represents the total number of firing angle is defined at each step.

The Fourier series for periodic wave forms provides:

$$v(t) = \frac{a_0}{2} + \sum_{n=1}^{\alpha} \left(a_n \cos n\omega_0 t + b_n \sin n\omega_0 t \right) \quad (1)$$

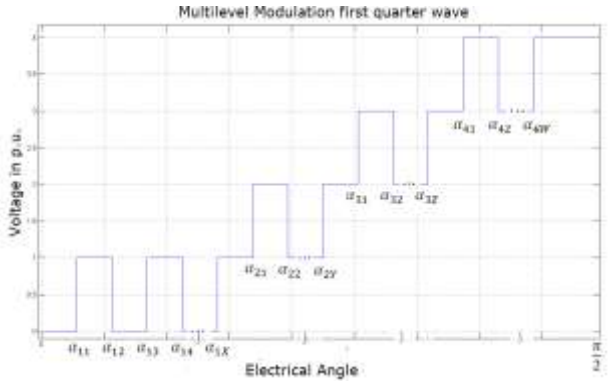

Fig. 5. Graphic of one quarter wave modulation regarding switch-on-and-off firing angles for each step.

Where, n is the harmonic number, ω the fundamental wave frequency, t the time, $a_0/2$ is the DC component, which is calculated by the expression:

$$a_0 = \frac{1}{2\pi} \int_0^{2\pi} v(\omega t)\, d(\omega t) \quad (2)$$

a_n coefficient of the Fourier series is calculated using (3):

$$a_n = \frac{1}{\pi} \int_0^{2\pi} v(\omega t) \cos n(\omega_0 t)\, d(\omega t) \quad (3)$$

b_n coefficient of the Fourier series , calculated by :

$$b_n = \frac{1}{\pi} \int_0^{2\pi} v(\omega t) \sin n(\omega_0 t)\, d(\omega t) \quad (4)$$

The waveform (Fig. 4) has odd symmetry and positive wave is equal to the negative, thus applying the symmetries of the theory of Fourier series.

$$a_0 = 0 \text{ y } a_n = 0 \quad (5)$$

Only be related coefficient with sinus, therefore, waveform in terms of the Fourier series will be expressed as follows:

$$v(t) = \sum_{n=1}^{\alpha} b_n \sin n\omega_0 t \quad (6)$$

b_n in terms of the vector L to the waveform :

$$b_n = \frac{4v_{cd}}{n\pi} \left\lfloor \sum_{i=1}^{4} \sum_{j=1}^{L_i} (-1)^{j-1} \cos n\alpha_{ij} \right\rfloor \text{ for } n \text{ odd}; \quad (7)$$

And $b_n = 0$ for n pairs.

Where i is the number of stage (hence the summation is from 1 to 4), L_i component i of vector L and α_{ij} the angle j of stage i, and this can be on or off. To obtain a ladder components vector L must be odd. If the peak magnitude of the harmonic n, in the Fourier series is defined as:

$$h_n = \sqrt{a_n^2 + b_n^2} \quad (8)$$

Substituting (5) and (7) to (8) the peak magnitude of each harmonic n is obtained, when only exist odd harmonic because $b_n = 0$ if n is pair, so:

$$h_n = \frac{4v_{cd}}{n\pi} \left\lfloor \sum_{i=1}^{4} \sum_{j=1}^{L_i} (-1)^{j-1} \cos n\alpha_{ij} \right\rfloor \text{ for } n = 1, 3, \ldots, \quad (9)$$

The standard IEEE 519 in 1992 [27], defines the total harmonic distortion as using (10):

$$THD = \frac{\sqrt{\sum_{n=2}^{50} h_n^2}}{h_1} \cdot 100 \quad (10)$$

Where h_1 is the fundamental harmonic component and h_n peak harmonic n.

Replacing (9) to (10):

$$THD = \frac{\sqrt{\sum_{n=2}^{50} \left[\frac{1}{n} \left(\sum_{i=1}^{4} \sum_{j}^{L_i} (-1)^{j-1} \cos n\alpha_{ij} \right) \right]}}{\left(\sum_{i=1}^{4} \sum_{j}^{L_i} (-1)^{j-1} \cos \alpha_{ij} \right)} \cdot 100 \quad (11)$$

Where n takes only odd values and L_i components vector $L = [x\ y\ z\ w]$. Thus (11) defines the objective function to be minimized by the optimization algorithm.

5 Optimization Algorithm

Using Matlab® and *Genetic Algorithm* Toolbox (GA), algorithms for the mathematical model of the fitness function (equation 11) and the corresponding optimization using genetic algorithms [28] were scheduled. The population size for the algorithm is taken from 20 individuals, each individual (X) formed by the total angle shot in the first quarter output voltage wave form:

$$X = \lfloor \alpha_{11}\alpha_{12} \cdots \alpha_{1x}, \alpha_{21}\alpha_{22} \cdots \alpha_{2y}, \alpha_{31} \cdots \alpha_{3z}, \alpha_{41} \cdots \alpha_{4w} \rfloor \quad (12)$$

The vector L, program to evaluate the fitness function angles corresponding to each step (flowchart shown in Figure 6).

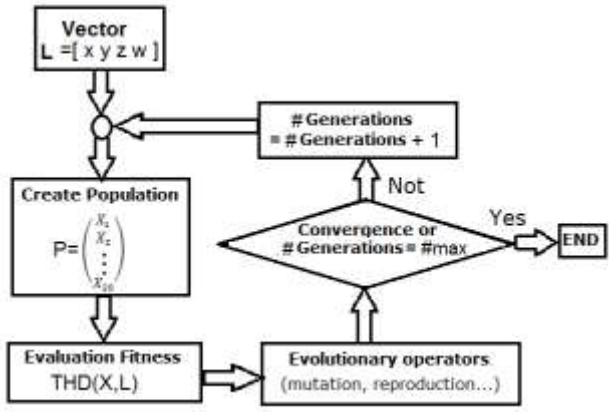

Fig. 6. Flowchart of the optimization genetic algorithm (GA).

The condition of algorithm was finished when the values of the population converge or because the number of generations reaches the maximum assigned.

5.1 Results

Figure 7 shows the evolution of the algorithm is shown below:

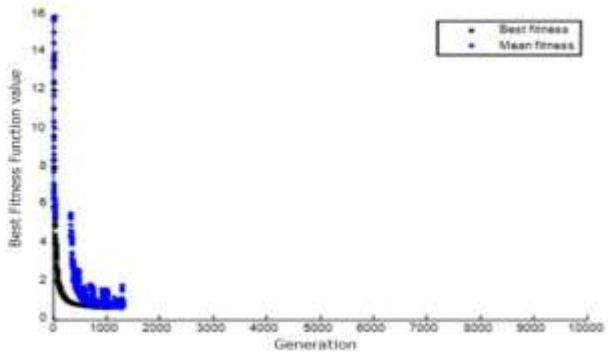

Fig. 7. Evolution of the genetic algorithm.

The modulation has found the following number vector angles in steps L = [3 5 5 11]. The individual with better fitness is presented in Table I, corresponding to the vector L defined above.

TABLE I. Angles in degrees of the best individuals.

x=3	y=5	z=5	w=11	
4.73702	19.02595	31.53636	53.98341	69.30872
7.04851	21.24552	33.92124	55.63071	70.78062
9.43937	23.98322	38.16271	59.44358	75.93116
	29.94251	41.60589	62.51731	76.61193
	31.53636	43.39352	65.04481	82.19461
				82.38271

The fitness for this individual, its THD, was calculated equal 0.2207 %. The output voltage waveforms of the modulation with these angles are shown in Fig. 8.

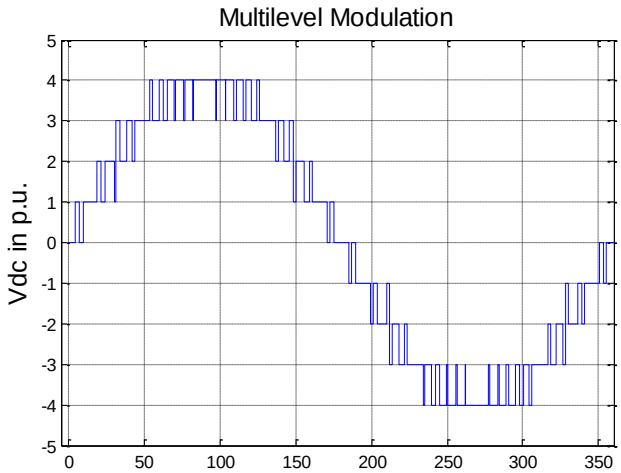

Fig 8. The output voltage waveform optimized modulation.

6 Simulation

The topology MLICH Bridge with common source described in Section 3, adopting found modulation was simulation using Simulink® Matlab® and using block Fast Fourier Transform (*FFT*) was obtained spectrum and the values of total harmonic content for different bands. The scheme of the simulation (Figure 9).

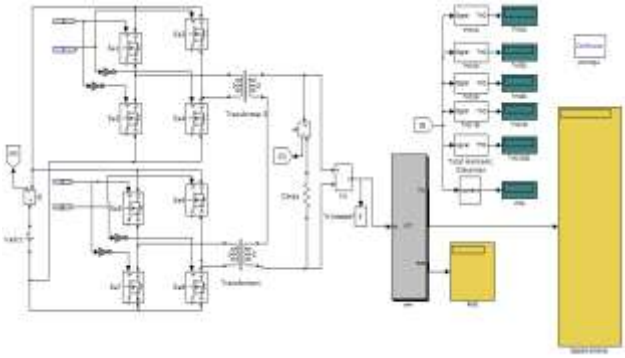

Fig 9. Simulink block diagram of the simulation inverter.

Figure 10 shows the waveform of the output voltage of the inverter and figure 11 the harmonic spectrum peak value, in this displacement of harmonic content is clearly observed at the higher harmonic frequencies 50, just as the *y*-axis (peak voltage) was expanded to observe the small presence at low frequencies, the maximum value the 15 harmonic (h_{15}) contribution to 0.21V, insignificant value when compared to the 180 V of the fundamental component (h_1).

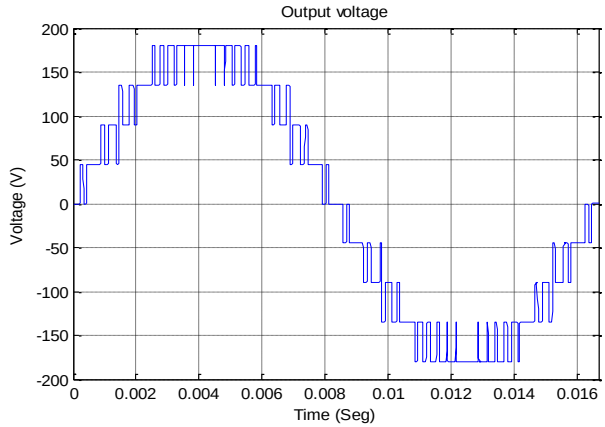

Fig. 10. Waveform output voltage inverter in the simulation.

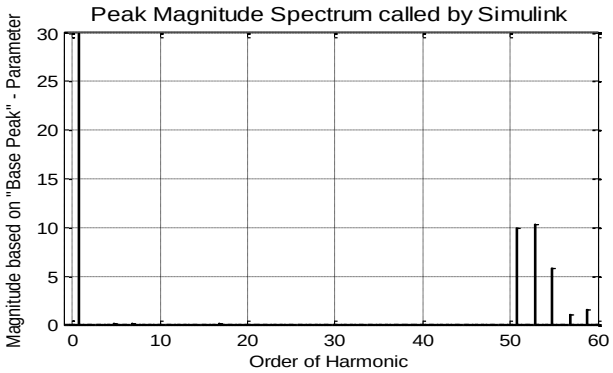

Fig. 11. Extending the spectrum of the output waveform (simulation).

The total harmonic distortion in the bands THDxx assessment (the number next to it indicates the harmonic THDv is evaluated), with the band THD50 defined for total harmonic distortion by the IEEE -519, are summarized in table II.

TABLE II. THDv in different bands evaluation.

%THD40	%THD50	%THD80
0.0	0.2207	11.16

Similarly values current were measured when the inverter fed a resistive load, the harmonic content to the component evaluated was THD_i 10 000 = 0.3 %, when assessed in the side THD50i the value is zero.

7 Prototype development

To validate results was implemented a low-power prototype, based on the use of MOSFETs as switching devices topology. Inverter output is 120 VA nominal input voltage 24 Vdc, so they apply to low cost photovoltaic systems, in which only a battery block is accumulator has the nominal frequency 60 Hz, and nominal output voltage of 120V rms. Drive control is performed only four signals necessary to control the upper MOSFETs of the bridges, the lower mosfet are controlled by the denial of the 4 signs of control and assigned died time was performed with hardware. The prototype was based on the use of FPGAXUPV5 - LX110T and final prototype in the dsPIC 30F4013. The transformer design, device critical in achieving waveform, it is raised according to an optimization proposed by the authors [16] that is to replace, in conventional methodologies transformer design , the equation:

$$\frac{N}{V_{rms}} = \frac{10^8}{2\pi \cdot f \cdot A\left[cm^2\right] \cdot B_{\max}\left[Gauss\right]} \tag{13}$$

For equation:

$$\frac{N}{V_p} = \frac{\left(\alpha_2 - \alpha_1\right) \cdot 10^8}{2\pi \cdot f \cdot B_{\max}\left[Gauss\right] \cdot A\left[cm^2\right]} \tag{14}$$

Where α_1 and α_2 are the angles that define the longer pulse input at transformer, or in the case because the initial and final angles of a pulse train that could saturate the transformer core. This improves the output waveform and reduces the load current of the transformer. In figure 12 shows the experimental prototype with FPGA.

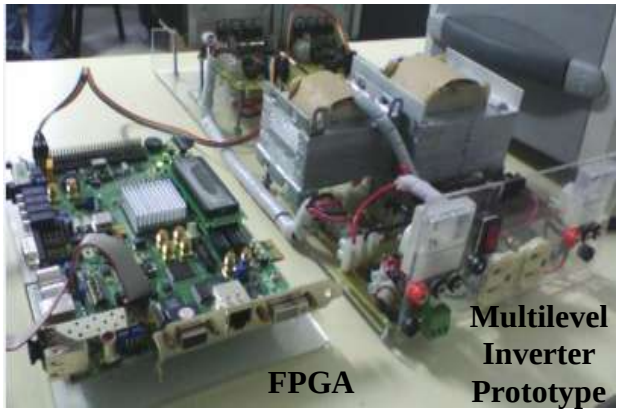

Fig. 12. Experimental prototype with FPGA.

8 Experimental set-up

In figure 16 assemblies was performed, shown equipment used in the tests. The output voltage and current of the inverter is evaluated through a data acquisition system (to evaluate the power quality) based on the acquisition card NI 6009 of the National Instruments with a sampling rate of 48Ks/s, evaluation software is programmed in Labview®, just as the data acquired voltage and current were processed in Matlab® Simulink® with FFT blocks. In both programs were evaluated harmonic contents, calculating the THD spectrum in the bands of 40, 50, 80 and 100 first harmonics; THD50 being the most representative shown standardized by IEEE-519.

Fig 13. Workstation with FPGA experimental tests.

Waveforms on the oscilloscope were observed and the rms values of current and voltage output test without load, with resistive load and inductive load is measured. In figure 14 a photograph of the shape of waves and Labview shown on the oscilloscope.

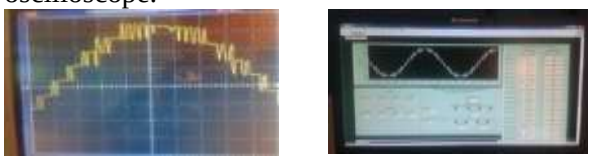
Fig. 14. Voltage on the oscilloscope and the evaluation system.

9 Results

The captured waveform Labview® for a test without load is shown in figure 15.

Fig. 15. Voltage to the inverter output.

The value calculated by the peak magnitude in Labview® (until the component 80) with the captured data, to a fundamental frequency of 60Hz spectrum is shown in figure16 and the evaluation by the Matlab® given captured data as results the voltage waveform of figure 17.

With the FFT block of Matlab® Simulink® for resistive load test the following harmonic spectra was obtained.

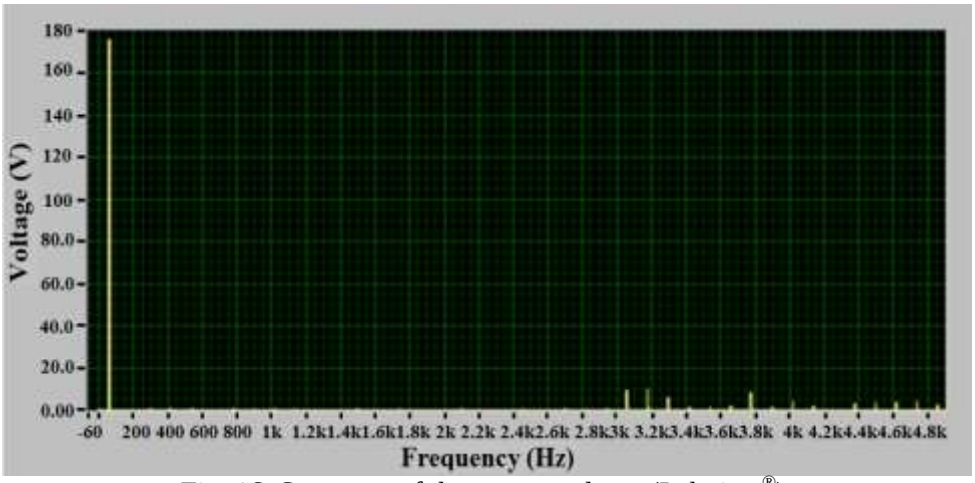

Fig. 16. Spectrum of the output voltage (Labview®).

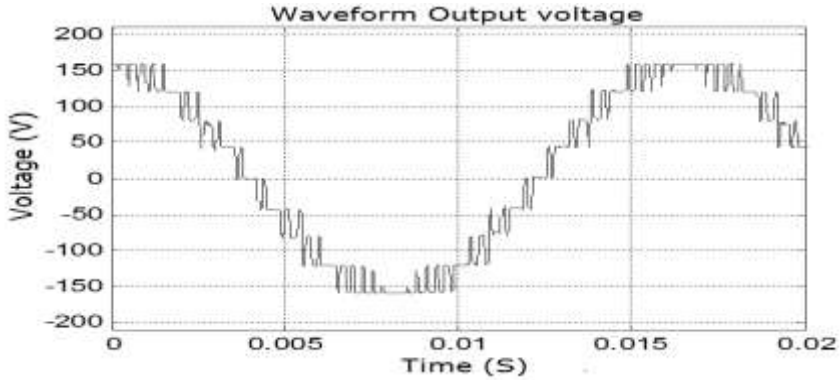

Fig. 17. Inverter Output voltage waveform-Matlab®.

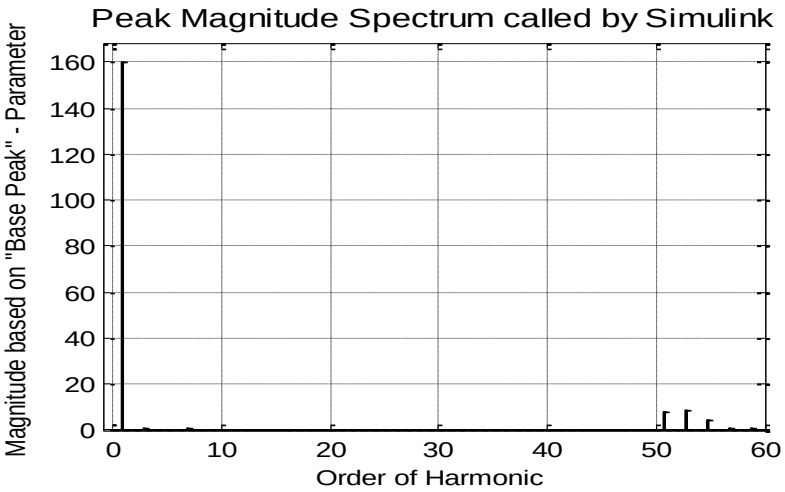

Fig 18. Spectrum of the output voltage in Matlab®.

Comparing the results of the two softwares used to assess the characteristics of harmonic content, it was observed that the behaviors are almost identical appearing on small differences, less 0.9%. Usually the harmonic content was always lower in Matlab® evaluation, and the minimum difference from Labview®.

The result of the tests and evaluations in the different bands of THDs is shown in table III. The highest values that are delivered by the evaluation system were taken.

TABLE III. Bands in different experimental THD.

Test	Vrms(V)	%THD40	%THD50	%THD80	%THD100
1	125.85	0.64	0.7062	11.26	12.17
2	115.89	0.925	0.96	10.49	11.2245
3	117.47	0.915	0.9448	11.3368	12.2567

Where: 1- Non-load test. 2 - Resistive load. 3- Inductive load.

The results validate the optimization performed in the range of 50 harmonics, appearing a THD = 0.96 % for the output voltage waveform. Similarly one can show that the behavior of the inverter is satisfactory, because although the calculated level is not reached, the THD is below 1 %, provided wide the standards proposed by the IEEE-519 standard 1992 set a limit of 5 %. Finally in figure 19 inverter operation is evidenced in its finished prototype, with the batteries block of a photovoltaic power low system.

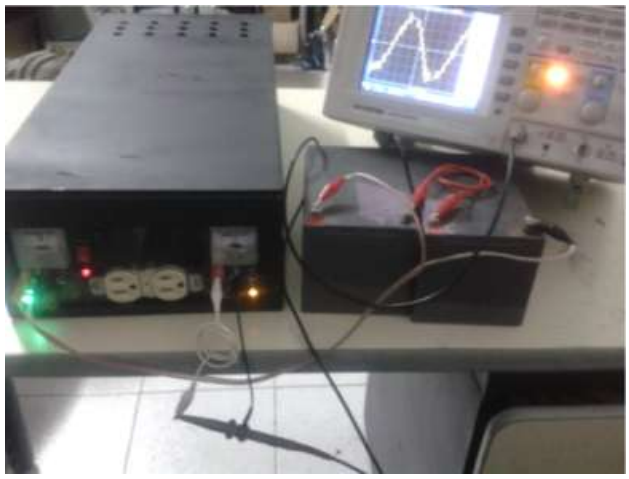

Fig. 19. Inverter operating with the photovoltaic system.

10 Conclusions

Simulations validated that the calculated TDH expression defined by the IEEE-519, for a multi - modulation PWM nine steps, is correct, since the spectra and THD values match with those values in the simulation algorithm.

The optimization algorithm developed will be able to void all harmonic content defined between 2 and 50 if given a sufficient number of shooting angles, however, it may be possible to find modulations that are not likely to implement.

The optimized theoretical THD for this project is defined as 0.2207 % which is the harmonic content of the modulation harmonic, optimized up to the 50 harmonic, this being the upper bound of assessment established by the IEEE 519.

The inverter performance shows the presence of voltage waveforms corresponding to those calculated in the optimization algorithm, it validates the transformer design proposed for such

applications, as well as the proposal to control the two-stages inverter with only four signals (2 for bridges), this was achieved by negating and allocation dead time for hardware, so it was possible to test, decreasing the software complexity and increasing performance.

From the experimental point of view the optimized THD, specifically for the voltage wave is defined as 0.96 % because this is the largest THD in the voltage waveform present in the harmonic modulation optimized up to the 50 harmonic.

To supply the in CHBMI with a photovoltaic power source system can significantly improve the power quality of these systems.

References

[1] Spertino, F.; Di Leo, P.; Corona, F.; Papandrea, F. "Inverters for grid connection of photovoltaic systems and power quality: Case studies" Power Electronics for Distributed Generation Systems (PEDG), 3rd IEEE Int. Symposium on Aalborg, June 2012, pp. 564 – 569.

[2] Hassan, A. and Mohamed, C. "Robust Controller for Interleaved DC-DC Converters and Buck Inverter in Grid-Connected Photovoltaic Systems" (APPEEC), WSEAS Transactions on Power Systems Vol. 6, 2011. pp. 21-30.

[3] Mohammad, S. Z.; Omar, A. N.; Andrahim, I. R. "A Review of Single-Phase Single Stage Inverter Topologies for Photovoltaic System". 4th Control and System Graduate Research Colloquium, Shah Alam, Malaysia, Vol. 19, N. 20, Aug. 2013, pp. 69-75.

[4] Mehmet, Y.; Seydi, V.; Seci, V. and Hasan, C. "Comparison of Output Current Harmonics of Voltage Source Inverter used Different PWM Control Techniques". WSEAS Transactions on Power Systems Volume 3, 2008. pp. 696-703.

[5] Karuppanan P. and Kamalakanta M. "PI, PID and Fuzzy Logic Controlled Cascaded Voltage Source Inverter based Active Filter for Power Line Conditioners" WSEAS Transactions on Power Systems Vol. 6, 2011 pp. 100-109.

[6] Longhua, Z.; Qing, F.; Xiangfeng, L.; y Changshu L. "A novel photovoltaic grid-connected power conditioner employing hybrid multilevel inverter" Sustainable Power Generation and Supply, SUPERGEN '09. International Conference on Nanjing, 2009, pp. 1-7.

[7] Rodriguez, J.; Jih-Sheng Lai; Fang ZhengPeng. "Multilevel inverters: a survey of topologies, controls, and applications". IEEE Trans. on Ind. Elect., Vol. 49, N. 4, 2002, pp. 724- 738.

[8] Rahim N.; Krismadinata; Wooi, H.; Selvaraj, J. "Elimination of Harmonics in Photovoltaic Seven-level Inverter with Newton-Raphson Optimization", Procedia Environmental Sciences, Volume 17, 2013, pp. 519-528.

[9] Debnath, S and Narayan, R. "THD Optimization in 13 level photovoltaic inverter using Genetic Algorithm". International Journal of Engineering Research and Applications. Vol. 2, Issue 3, May-Jun 2012, pp. 385-389.

[10] Ríos, F. and Dixon J. Diseño y construcción de un inversor trifásico multinivel. Trabajo de Grado, Pontificia Universidad Católica de Chile, Santiago de Chile, 2003.

[11] Baker R. H. and Lawrence H. B. Electric Power Converter, US. Patent Number: 3,867,643, 1975.

[12] Nabae, A. , Takahashi, I. y H. Akagi. "A new neutral point clamped PWM inverter", IEEE Trans. Ins. Appl., vol. IA-17, N. 5, pp.518-523, Sep-Oct 1981.

[13] Malinowski, M.; Gopakumar, K.; Rodriguez, J. and Pérez, M. "A Survey on Cascaded Multilevel Inverters", IEEE Trans. on Ind. Elect., Vol. 57, N. 7, July 2010, pp. 2197-2206.

[14] Panda, A. K. and Suresh, Y. "Research on cascade multilevel inverter with single DC source by using three-phase transformers". Int. Journal of Electrical Power & Energy Systems, Vol. 40, N. 1, 2012, pp. 9-20.

[15] Banaei, M. R.; Khounjahan H. y Salary, E. "Single-source cascaded transformers multilevel inverter with reduced number of switches". IET Power Electron, Vol. 5, N. 9., 2012, pp. 1748-1753.

[16] Diaz R., J. L.; Pabón, L. D.; and Caicedo, A. "Optimization to improve power quality in the design of transformers for power multilevel inverters". Universidad de Pamplona, 2014.

[17] Govindaraju, C. and Baskaran, K. "Performance Improvement of Multiphase multilevel Inverter Using Hybrid Carrier Based Space Vector Modulation". International Journal on Electrical Engineering and Informatics - Vol. 2, N. 2, 2010.

[18] Karuppanan, P. and Mahapatra, K. "FPGA based cascaded multilevel pulse width modulation for single phase inverter," Environment and Electrical Engineering (EEEIC), 2010 9th International Conference on, Vol. 16, N. 19, Mayo 2010, pp. 273-276.

[19] Al-Judi, A.; Bierk, H. and Nowicki, E., "Selective harmonic power optimization in multilevel inverter output" Vehicle Power and

Propulsion Conference (VPPC), Vol. 6, N. 9, Sept. 2011, pp. 1-5.

[20] Periasamy, M. and Shankar, M. "Harmonic optimization of cascade multilevel Inverter with unequal DC sources using genetic algorithm". International Journal of Engineering Research & Technology, Vol. 1, N. 6, August, 2012.

[21] Mathew, M. "THD Reduction in Multilevel Inverters Using Real-Time Algorithm". Journal of Computer Engineering, Vol. 8, N. 2, Nov.-Dec. 2012, pp. 1-12.

[22] Yousefpoor, N.; Fathi, S.H.; Farokhnia, N. and Abyaneh, H.A., "THD Minimization Applied Directly on the Line-to-Line Voltage of Multilevel Inverters," IEEE Transactions on Ind. Elect., Vol. 59, No.1, Jan. 2012, pp. 373-380.

[23] Narayan, R.; Chatterjee, D. and Kumar, S. "A PSO based optimal switching technique for voltage harmonic reduction of multilevel inverter", Expert Systems with Applications, Vol. 37, N. 12, Dec. 2010, pp. 7796-7801.

[24] Papriwal, A. and Mahor, A. "Review of mitigation of harmonics in multilevel inverters using PSO" International Journal of Electrical and Electronics, Vol. 2, N. 4, Dec. 2012, pp. 65-72.

[25] Araque G., J. A.; Diaz R., J. L. and Pardo G., A. "Optimization of the THD in a Multi-Level Single-Phase Converter using Genetic Algorithms". Advances in Automatic Control, Modelling & Simulation WSEAS Conference Brasov 2013, pp. 326-331.

[26] Debnath, S. Narayan, R. and Ghosh, T. "Comparison of Different Soft Techniques applicable to Multilevel Inverter for Harmonic Elimination". International Journal of Computer Application, Vol. 6, N. 2, Dec., 2012.

[27] IEEE Std. 519-1992 - IEEE Recommended Practices and Requirements for Harmonic Control in Electrical Power Systems. IEEE, 1992.

[28] Goldberg, D. E. "Genetic Algorithms in Search, Optimization and Machine Learning". Addison-Wesley Publishing Company, 1989.